CrossMark

Effect of a novel polysiloxane-containing nitrogen on the thermal stability and flame retardancy of epoxy resins

Le Zhang[1] · Youchuan Wang[1] · Xufu Cai[1]

Abstract A novel polysiloxane-containing nitrogen (PSiN) was synthesized, and it was added to epoxy resin (EP) as flame retardant. The structure of PSiN was characterized by Fourier transform infrared spectroscopy and ^{1}H NMR. The effect of PSiN on the flame retardancy and thermal behaviors of EP were investigated by limited oxygen index (LOI), microscale combustion calorimetry test (MCC) and thermogravimetric analysis (TG). The results showed that the flame retardancy and the thermal stability of EP were improved with the addition of PSiN. When 4.5 mass% PSiN was incorporated, the LOI value of EP was found to be 29 %, which is higher than 21 % of pure EP. The char structure observed by scanning electron microscopy (SEM) indicated that the surface of the char for EP100/DDM (4,4-diaminodiphenyl-methane) 20.7/PSiN4.5 system holds a smoother and denser char structure when compared with EP100/DDM21.8 and EP100/PSiN90 systems.

Keywords Organic silicon · Epoxy resins · Flame retardant · Thermal stability · Curing

Introduction

Epoxy resins(EPs) are widely used in the area of adhesives, coatings and advanced composites of the aerospace and electronics industries, because of their mechanical stiffness, toughness, superior adhesion, modulus, good chemical and corrosion resistance and excellent dimensional stability [1, 2]. EPs have a dominant position in the development of high-performance materials. However, the epoxy resins are difficult to satisfy the requirements of special engineering technology with the index (LOI) of 19.8 %, which limits the application of epoxy resin in many important areas, so the flame retardancy of EP needs to be improved [3–5].

Although halogen flame retardants have good flame-retardant effect on epoxy resins, the flame retardants would produce a large amount of toxic and corrosive smoke in combustion process [6]. So, low-smoke and halogen-free flame retardants of epoxy resin have attracted increasing attention [7–9]. Among them, silicone-containing epoxy flame retardants will be one of the choices [10]. Silicon element is considered to be an environmentally friendly flame retardant because it can reduce the harmful impact on the environment more than the existing materials [11–13].

Researches have shown that the addition of relatively small amounts of silicon compounds to various polymeric materials can improve their flame retardancy [14, 15]. And introducing silicon element and its groups into epoxy can also improve some other properties of the epoxy resins, such as thermal stability, high resistance to thermal oxidation, low surface energy and low toxicity [16–18]. The conventional practice of introducing siloxane compounds into polymers has been achieved by blending those polymers with polydimethylsiloxanes [19]. But problems such as poor compatibility, leaching and reduced mechanical properties limit their application. In order to reduce the above limitation, the silicone elements or groups are incorporated into the epoxy resin backbone [20–23].

In this work, a novel organic silicon flame-retardant containing silicon and nitrogen (PSiN) was synthesized and

✉ Xufu Cai
  caixf2008@scu.edu.cn

[1] Department of Polymer Science and Engineering, Sichuan University, Chengdu 610065, China

Springer

it was added to epoxy resins. This organic silicon flame retardant carrying silicon and amino (PSiN) can introduce silicon into the epoxy resin backbone. The compatibilization, thermal degradation behavior and the flame-retardant effect were investigated by thermogravimetric analysis (TG), differential thermogravimetric analysis (DTG), microscale combustion calorimetry test (MCC), scanning electron microscopy (SEM), differential scanning calorimetry (DSC) and limiting oxygen index (LOI).

Experimental

Materials

Diglycidyl ether of bisphenol A (DGEBA, EP, epoxy value = 0.44 mol/100 g) was supplied by Wuxi Bluestar Chemical Co., Ltd., China. N-(β-aminoethyl)-γ-aminopropylmethyldimethoxysilane (KH-602) and dimethoxydimethylsilane were provided by Nanjing Union Silicon Chemical Co., Ltd. (Nanjing, China), and Bluestar Chemical Research Institute (Chengdu, China), respectively. 4,4-Diaminodiphenyl-methane (DDM) was supplied by Chengdu Kelong Chemical Reagent Factory.

Synthesis of PSiN

A 250-mL three-necked round-bottom flask equipped with a stirrer, a thermometer and a condenser was charged with 12 g (0.1 mol) dimethoxydimethylsilane, 20.6 g KH-602 (0.1 mol) and 5 g H_2O. Then, a suitable amount of ammonia was added into the flask as catalyst. After being maintained at room temperature for 20 min, the solution was heated to 60 °C with stirring for 4.5 h. After being cooled to room temperature, the raw product was washed by ethanol and n-hexane to remove the residual KH-602. The product was dried in a vacuum at 110 °C. The synthesis route is illustrated in Fig. 1.

Preparation of flame-retardant EP samples

Various compositions of EP systems were prepared as the following steps. First, appropriate amount of epoxy was
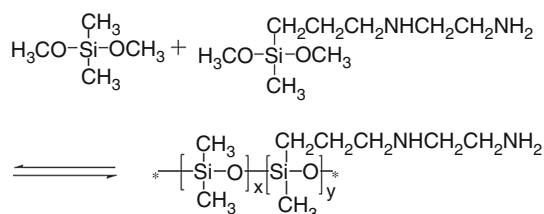
stirred at 60 °C. Second, stoichiometric DDM was casted into the blend above to dissolve at 100 °C. Third, the appropriate amount of PSiN and DDM was put into the epoxy. Compositions of the EP are shown in Table 1. With the increase of PSiN-containing amino group, the DDM is reduced, so that the mole of active hydrogen is constant in the system. The PSiN-cured EP scheme is shown in Fig. 2. Subsequently, the blend was put into a mold for curing and post-curing at oven as the following procedure: 80 + 120 + 150 °C/2 h. The thickness of the mold was 3 mm. The blend molded into standard testing bars for further test.

Instrumental analyses

FTIR spectroscopy was applied with a Nicolet IS10 Fourier transform infrared (FTIR) spectrometer using KBr pellets. ^{1}H NMR (400 MHz) spectrum was recorded on a FT-80A NMR using $CDCl_3$ as the solvent. The Q-200 (TA Instrument) was used for differential scanning calorimetry (DSC) under nitrogen atmosphere using a scanning rate of 10 K min^{-1}. LOI data of all samples were obtained at room temperature on an oxygen index instrument (XYC-75) produced by Chende Jinjian Analysis Instrument Factory, according to GB/T 2406-93 standard. The dimensions of all samples were $130 \times 6.5 \times 3$ mm^3. LOI was an important parameter for evaluating the ease of extinguishment of polymeric materials in the same condition. It denotes the lowest volume concentration of oxygen sustaining candle burning of materials in the mixing gases of nitrogen and oxygen. Thermogravimetric analysis (TG) was performed on a Mettler-Toledo instrument TG/DSC1 at a heating rate of 10 °C min^{-1}. About 10 mg of the sample was examined under pure nitrogen or air condition at a flowing rate of 60 mL min^{-1} at temperatures ranging from 30 to 800 °C. The surface morphology of the char obtained after the LOI test was observed by scanning electron microscopy (SEM).

Fig. 1 Synthesis of PSiN

Table 1 Compositions of the EP systems

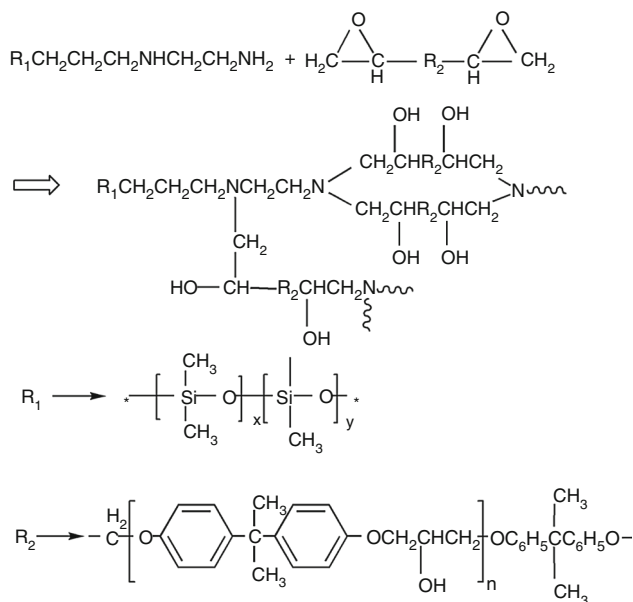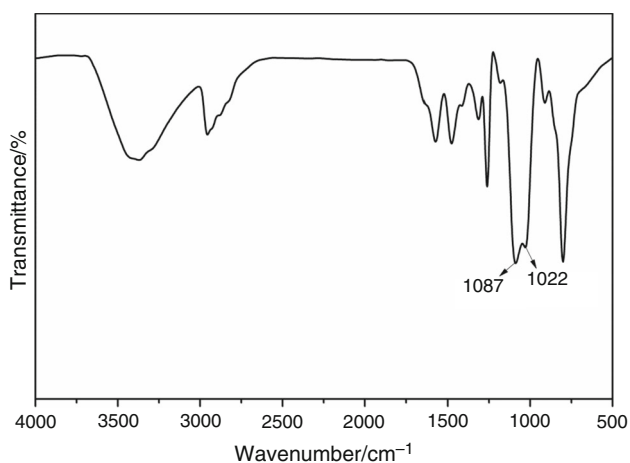| Sample	Components/mass/%		
	E-44	DDM	PSiN
1	100	21.8	–
2	100	–	90
3	100	10.9	45
4	100	17.4	18
5	100	19.6	9
6	100	20.7	4.5
7	100	21.3	2.25

Fig. 2 PSiN-cured EP scheme

Fig. 3 IR spectrum of PSiN

Results and discussion

Characterization of PSiN

Figure 3 shows the FTIR spectrum of the synthesized PSiN. The absorption bands at 2960 cm^{-1} correspond to vibrations of C–H. The peaks at 1022 and 1087 cm^{-1} are associated with the vibrations of Si–O–Si. The absorptions at 1260 and 800 cm^{-1} are assigned to Si–CH$_3$. The absorptions at 1476 cm^{-1} are assigned to –CH$_3$, –CH$_2$. The peaks at 3356 cm^{-1} are associated with the vibrations of –NH$_2$. The information above confirms that the target product was synthesized successfully.
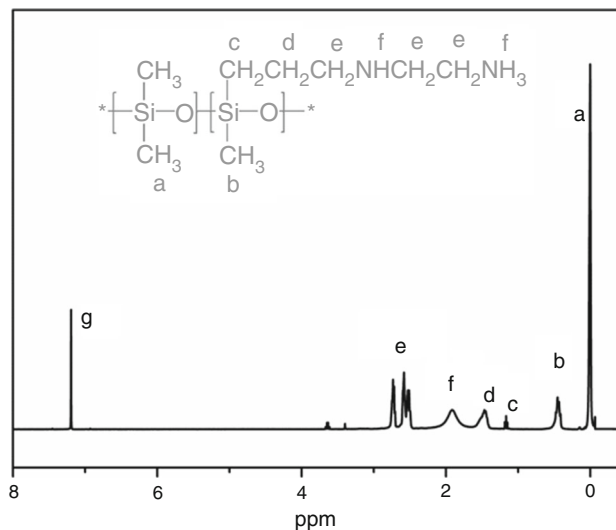

Fig. 4 ^{1}H-NMR spectrum of PSiN

So as to further determine the structure of PSiN. Figure 4 shows that the ^{1}H NMR spectrum of PSiN (ppm): 0.04 ppm (CH$_3$–Si–CH$_3$), 0.5 ppm (Si–CH$_2$–), 1.3–1.6 ppm (–Si–CH$_2$–CH$_2$–N–), 1.8–2.1 ppm (–NH), 2.5–3.0 ppm (N–CH$_2$) and 7.2 ppm is the CDCl$_3$. All these characteristic ^{1}H NMR bands indeed match the PSiN structure. These suggest that PSiN is successfully processed. On the other hand, the molar ratio (X:Y) of dimethyldimethoxysilane to KH602 was determined by the ratio of the area of peak a (–CH$_3$ in dimethyldimethoxysilane) to that of peak f (–NH in KH602), and the result indicates the value of X:Y is 1.

Differential scanning calorimetry (DSC)

Usually, the variation of siloxane content will affect glass transition temperatures of the blending system [24]. Figure 5 shows DSC curves of cured EP systems. All of the mixed epoxy systems exhibit single glass transition temperature (T_g). It is well known that an absolutely miscible blend presents only one T_g peak. This single T_g phenomenon indicates a homogeneous morphology of these hybrid epoxy systems. It can be seen that the EP100/PSiN90 gives the lowest T_g (106 °C), while the EP100/DDM21.8 gives the highest T_g (155 °C). The rest of the mixed epoxy systems also exhibit single T_g between 106 and 155 °C. This phenomenon can be mainly interpreted by the fact that the chemistry of EP100/PSiN90 differs from that of EP100/DDM21.8. The latter has rigid chain. With the decreasing of the content of PSiN, the T_g becomes more and more higher. This is because that PSiN contains much Si–O–Si which increases the flexibility and movement of the chain.
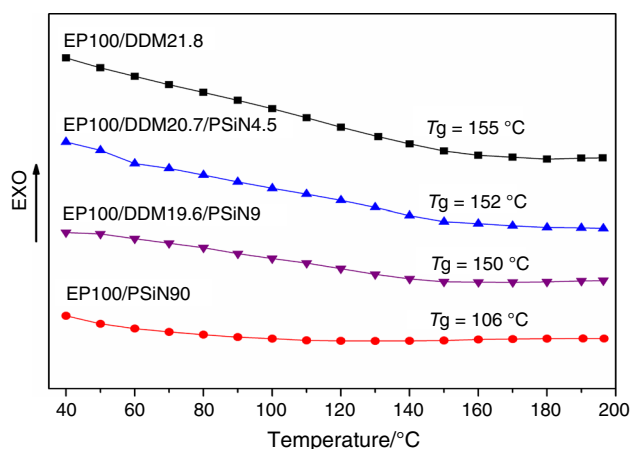
Fig. 5 DSC curves of finally cured products

Fig. 6 Heat release rate curves versus temperature

Flammability

The flame retardancy of EP systems was evaluated by measuring their LOI values. Data are listed in Table 2. It is clear that a significant increase in LOI (from 21 to 29 %) was observed when PSiN was utilized in the epoxy systems. When the DDM of the EP was 20.7 mass% and PSiN was 4.5 mass%, the LOI of the EP system reached a maximum of 29 %. At the same time, the addition of PSiN will produce less smoke in the combustion process. These results proved that there was a synergistic effect of DDM and PSiN when they were added to EP. In addition, the LOI of EP system, the PSiN being used as the curing agent, is higher than that of the EP system with PSiN being added just as the flame retardant. It can be proved that the LOI of sample 6 (S6) is higher than that of the S8. This may be due to PSiN-contained amino group, so the curing agent of S8 is excessive when PSiN was added just as flame retardant, which lead to a lower cross-linking degree, thus the lower LOI.

Microscale combustion calorimetry test

The heat release rate (HRR), the peak heat release rate (PHRR), heat release capacity (HRC) and the total heat release (THR) are important parameters in quantitative material flammability analysis. The dynamic flammability data detected by microscale combustion calorimeter of EP and EP samples are shown in Fig. 6 and Table 3. Figure 6 contains curves of the heat release rate (HRR) of EP

Table 3 Combustion parameters obtained from MCC

Sample	PHRR/W g^{-1}	THR/kJ g^{-1}	T_{PHRR}/ °C	HRC/J g^{-1}
1	467.5	22.9	392.1	472
6	415	22.6	405	427

systems. A sharp peak appeared in the HRR of EP100/DDM21.8 with a peak heat release rate (PHRR) of 467.5 W g^{-1}, while EP100/DDM20.7/PSiN4.5 showed a slower burning rate with the peak reduced to 415 W g^{-1}. The heat release capacity of EP100/DDM21.8 and EP100/DDM20.7/PSiN4.5 is presented in Table 3. The heat release capacity (HRC) of EP100/DDM20.7/PSiN4.5 was lower than EP100/DDM21.8. This lower HRC value indicates that a part of the EP system was not completely combusted, probably undergoing a carbonization process. It is believed that some char residue formed in the thermal decomposition process of EP, which could lead the heat release rates to decrease. This effectively improves the flame retardancy of the matrix.

Thermal analysis

The thermal stability of EP100/DDM21.8, EP100/PSiN90 and EP100/DDM20.7/PSiN4.5 resins was characterized by TG under nitrogen and air atmosphere. T_5 % represents the temperature at which mass loss is 5 % for the system (the initial decomposition temperature), T_{max1} represents the temperature of the first maximum mass loss rate for the system, T_{max2} represents the temperature of the second maximum mass loss rate for the system, and Y_c represents the char yields at 800 °C [25].

Figures 7 and 8 show the TG and DTG curves of cured EP100/DDM21.8, EP100/PSiN90 and EP100/DDM20.7/PSiN4.5 in nitrogen, respectively. It can be observed that
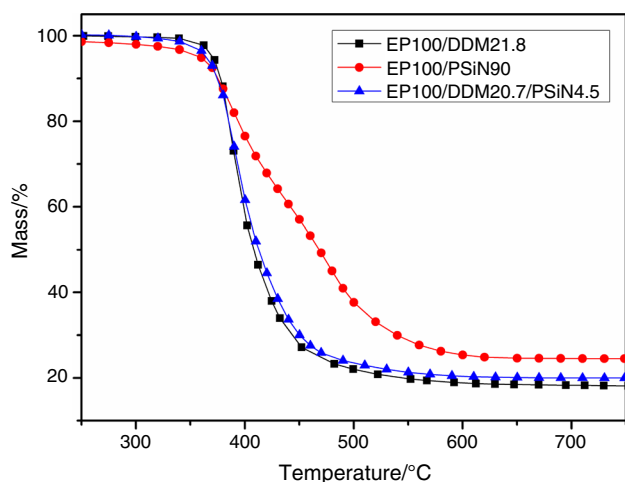
Table 2 Limiting oxygen indices of finally cured products

Sample	1	2	3	4	5	6	7
LOI/%	21	25.5	26	27	29	29	25.5

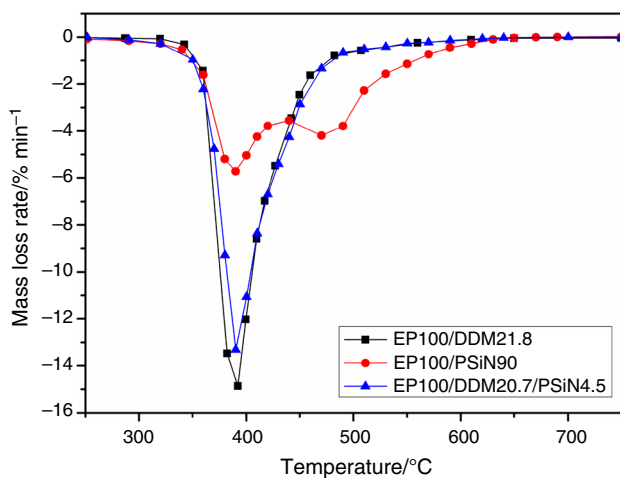Fig. 7 TG curves of finally cured products in N_2

Fig. 8 DTG curves of finally cured products in N_2

EP100/DDM21.8 and EP100/DDM20.7/PSiN4.5 have one-stage decomposition process. This dramatic mass loss was due to the decomposition of the resin matrix. However, EP100/PSiN90 has two-stage decomposition process. The two-stage mass loss results from the complicated decomposition of silane groups and the resin matrix, respectively. The decomposition of silane groups is able to form a silicon-rich residue after the initial stage of mass loss to slow down further decomposition of the resins. The T_5 % (the initial decomposition temperature) of EP100/PSiN90 and EP100/DDM20.7/PSiN4.5 resins is lower than that of EP100/DDM21.8 as shown in Table 4. Due to the initial decomposition of PSiN that occurs at inferior temperature, the Si–O group of PSiN is able to absorb more thermal energy and its vibration can dissipate the thermal decomposition energy [26]. The temperature of the maximum mass loss rate (T_{max}) of EP100/DDM21.8 is lower than that of EP100/PSiN90 and EP100/DDM20.7/PSiN4.5. This is caused by the phenomenon that the decomposition of PSiN at inferior temperature leads to the formation of the silicone-containing group, which will participate in the cross-linked carbonization. It can convert the usual organic decomposition to partially inorganic decomposition by forming the carbon–silicon residue to act as thermal insulation [27] and to prevent gas evolution, and achieve ultimate improvement on flame retardation of this silicone-containing epoxy system.

Figures 9 and 10 show the TG and DTG curves of cured EP100/DDM21.8, EP100/PSiN90 and EP100/DDM20.7/PSiN4.5 in air atmosphere, and the data from the curves are shown in Table 4. We can see that EP100/DDM21.8 and EP100/DDM20.7/PSiN4.5 resins have two decomposition stages, while EP100/PSiN90 has three-stage decomposition process. For EP100/DDM21.8 and EP100/DDM20.7/PSiN4.5 resin, the first thermal decomposition is occurred between 362 and 470 °C which was assumed as the thermal degradation of the polymer network and the second stage is from 500 to 700 °C which was assumed as the oxidation process of the char moiety. For the first stage decomposition of the EP100/PSiN90 in air atmosphere, the maximum mass loss rate occurs at a temperature of about 18 °C lower than that in nitrogen atmosphere. Therefore, the decomposition of PSiN starts at a lower temperature as the result of oxidation in breaking off the silicone-containing group. The carbonization mechanism dominates the second stage of EP100/PSiN90 and the first stage of EP100/DDM21.8, the former is about 90 °C higher than the latter. For decomposition at even higher temperatures corresponding to the third stage for EP100/PSiN90 and the second stage for EP100/DDM21.8, the temperature of maximum mass loss rate for EP100/PSiN90 is about 55 °C higher than that for EP100/DDM21.8. The introduction of this silicone-containing group into the epoxy structure is able to cause the cross-linked carbonization and results in higher oxidation temperature, and thus raises flame retardation significantly [28].

For decomposition either in air or in nitrogen atmosphere, the solid char yield at 800 °C for EP100/PSiN90 is significantly higher than that for EP100/DDM21.8. The higher char yield from the EP100/PSiN90 indicates that the carbonization mechanism indeed plays an important role in flame retardation [30]. The LOI value of the EP100/PSiN90 is 25.5, which is higher than that of the EP100/DDM21.8 at 21. For decomposition either in air or in nitrogen atmosphere, the solid char yield and the oxidation temperature of maximum mass loss rate in the third stage of EP100/PSiN90 were higher than that of EP100/DDM20.7/PSiN4.5. The LOI of EP100/PSiN90 is lower than EP100/DDM20.7/PSiN4.5. It may be attributed to the higher temperature of cross-linked carbonization results in the forming of char layer at the higher temperature.

Table 4 Thermal property of finally cured products

Sample	T_5 %/°C		T_{max1}/°C		T_{max2}/°C		R_{max}/% min^{-1}		Y_c/%	
	N$_2$	Air	N$_2$	Air	N$_2$	Air	N$_2$	Air	N$_2$	Air
1	371	370	383	380	–	599	16	16	18	0
2	359	355	389	371	476	476	5.7	6	25	22
6	365	351	391	382	–	606	13	11	20	2.3
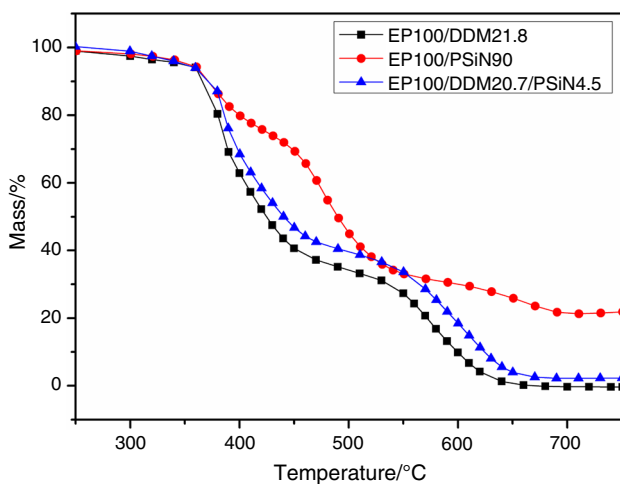
Fig. 9 TG curves of finally cured products in air
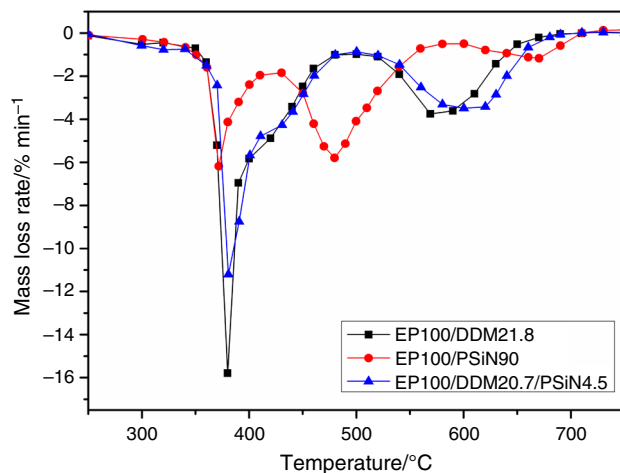
Fig. 10 DTG curves of finally cured products in air

Morphology of char residue by SEM

It was known that the effective protective char layer could improve the flame retardancy during combustion. To explore how the structure of char determines the flame retardancy of EP, the morphologies of the chars were examined by SEM. The SEM micrographs of the char residue of EP100/DDM21.8, EP100/PSiN90 and EP100/DDM20.7/PSiN4.5 are shown in Fig. 11a. It was found that there are many uneven holes on the surface of the residue, suggesting a poor char quality. This poor char layer cannot efficiently act as a barrier to shield the underlying polymer from heat and air. Figure 11b shows the SEM micrograph of EP100/PSiN90. The char is compact, smooth compared with a. However, due to lacking of the frame, this system burned into powder directly. As a result, oxygen cannot be isolated and this char cannot effectively prevent heat and matter to transfer. Figure 11c shows a compact, smooth and connective char; there was little flaw and lots of tight ball that can increase the thickness and density of carbon layer on the surface of the charred layer, resulting in insulating oxygen very well, which can effectively prevent the underlying polymer from the heat. So, the LOI value of EP100/DDM20.7/PSiN4.5 is found to be 29 %, which is higher than EP100/DDM21.8 and EP100/PSiN90.

Structural analysis of the combustion residue by FTIR

Figure 12 shows FTIR spectra of EP100/DDM20.7/PSiN4.5 system and its solid products collected in thermogravimetric at 800 °C. In the initial absorption of this system, the peaks at 3423, 2921, 1608, 1508, 1508, 1263 and 815 cm^{-1} are the characteristic absorption of epoxy resin networks [29], and the peaks at 1025 cm^{-1} are associated with the vibrations of Si–O–Si. At 800 °C, the absorption of aliphatic components disappears totally. Peaks at 1034 and 1590 cm^{-1} are observed in the spectrum of curve b. These peaks are attributed to the Si–O and condensed aromatic bonds, respectively.

To further clarify the structure of the flame-resistant barrier on the surface, the EP100/DDM21.8, EP100/PSiN90 and EP100/DDM20.7/PSiN4.5 were analyzed after combustion using infrared spectroscopy (IR). The IR spectra of those systems are shown in Fig. 13. Peaks at 1608, 1508 and 834 cm^{-1} are observed in the FTIR spectrum of the residue obtained from LOI testing of EP100/DDM21.8, which are attributed to the condensed aromatic bonds. Peaks at 3460, 1080 cm^{-1} are observed in the spectra of EP100/PSiN90 and
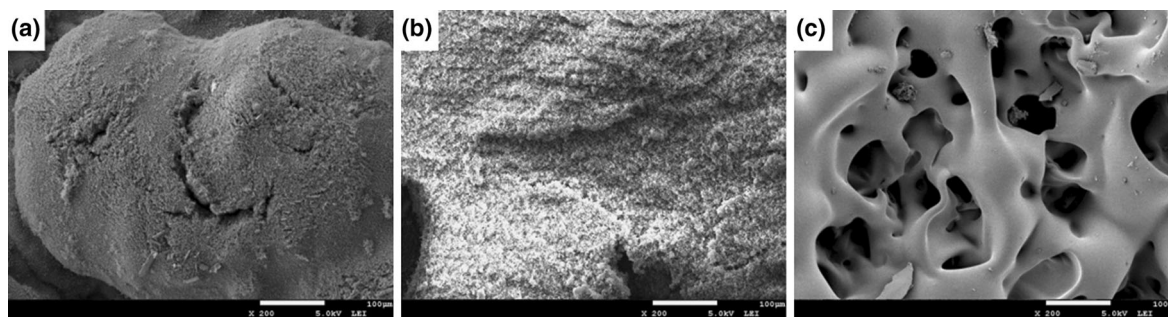
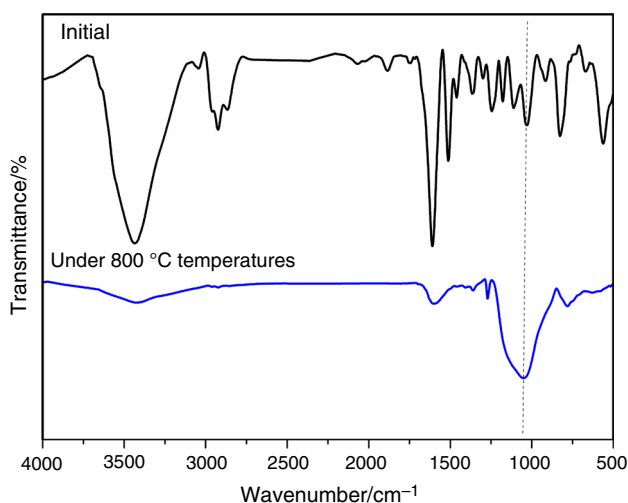**Fig. 11** SEM of the residual char: **a** EP100/DDM21.8, **b** EP100/PSiN90, **c** EP100/DDM20.7/PSiN4.5

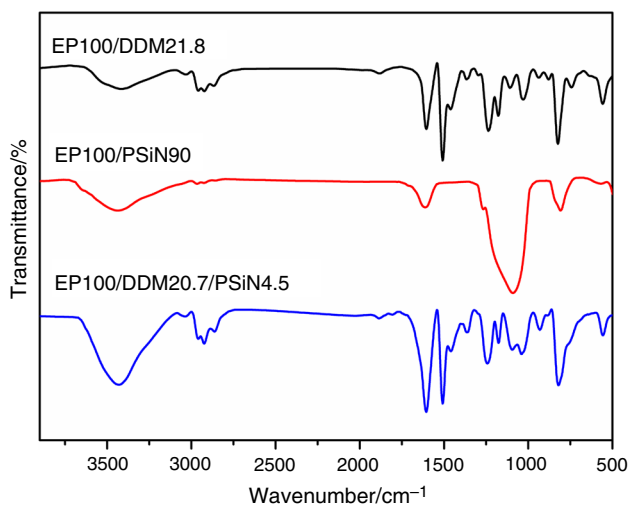**Fig. 12** FTIR spectrum of the condensed phase of EP/PSiN/DDM (sample 6)

Fig. 13 FTIR spectrum of the residue from burning

EP100/DDM20.7/PSiN4.5, while the peaks are not in the spectrum of EP100/DDM21.8. These may be attributed to the Si–O and –OH bonds, respectively. In the curve of

EP100/PSiN90, there is only one peak in 1600–1450 cm^{-1}, while in the curve of EP100/DDM20.7/PSiN4.5, the peak at 1608 cm^{-1} becomes broader than in EP100/DDM21.8, indicating the formation of silica ring. Based on the observed results for EP100/DDM21.8, EP100/PSiN90 and EP100/DDM20.7/PSiN4.5 systems, it is proposed that EP100/PSiN90 would form char residues which largely consists of silica ring, while EP100/DDM20.7/PSiN4.5 would form char residues with the matrix, which mainly consists of condensed aromatic compounds and Si–O units. This char layer can act as a barrier to shield the underlying polymer from heat and air.

Conclusions

A novel polysiloxane (PSiN) with amino groups was synthesized by dimethoxydimethylsilane and N-(β-aminoethyl)-ϒ-aminopropylmethyldimethoxy-silane (KH-602) and it was added to epoxy. Flame retardancy of EP was improved with the addition of PSiN. The LOI of EP100/DDM20.7/PSiN4.5 is 29. The TG curves demonstrated that the addition of organic silicon improves the amount of carbon residue and the thermal stability of EP. The char residues of EP100/DDM20.7/PSiN4.5 in N$_2$ could reach 20 mass% at 800 °C. In SEM micrographs, a compact, continuous char layer could be observed, and this slowed heat and mass transfer between the gas and condensed phases. The infrared (IR) spectrum of EP100/DDM20.7/PSiN4.5 after combustion showed that PSiN promotes the formation of the char on the surface of the polymer during combustion, which largely consists of condensed aromatic compounds and Si–O units. This char layer can act as a barrier to shield the underlying polymer from heat and air.

References

1. Liu Q, Bao X, Deng SQ. The investigation of methyl phenyl silicone resin/epoxy resin using epoxy-polysiloxane as compatibilizer. J Therm Anal Calorim. 2014;118:247–54.

2. Bao X, Cai XF. Synergistic effect of methyl phenyl silicone resin and DOPO on the flame retardancy of epoxy resins. J Therm Anal Calorim. 2014;118:369–75.

3. Ahmada S, Gupta AP, Sharmin E, Alam M, Pandey SK. Synthesis, characterization and development of high performance siloxane-modified epoxy paints. Prog Org Coat. 2005;54:248–55.

4. Wu CS, Liu YL, Chu YS. Epoxy resins possessing flame retardant elements from silicon incorporated epoxy compounds cured with phosphorus or nitrogen containing curing agents. Polym. 2002;43:4277–84.

5. Jiang J, Chen YB, Liu Y, Wang Q. Intergrowth charring for flame-retardant glass fabric-reinforced epoxy resin composites. J Mater Chem A. 2015;3:4284–90.

6. Yuan DD, Yin HQ, Cai XF. Synergistic effects between silicon-containing flame retardant and potassium-4-(phenylsulfonyl)-benzene-sulfonate (KSS) on flame retardancy and thermal degradation of PC. J Therm Anal Calorim. 2013;114:19–25.

7. Chen XL, Jiao CM. Synergistic effects of hydroxy silicone oil on intumescent flame retardant polypropylene system. Fire Saf J. 2009;44:1010–4.

8. Lu SY, Hamerton I. Recent developments in the chemistry of flame retardant composites matrices. Prog Polym Sci. 2002;27:1661–712.

9. Shen H, Wang YH, Mai KC. Non-isothermal crystallization behavior of PP/Mg(OH)$_2$ composites modified by different compatibilizers. Thermochim Acta. 2007;457:27–34.

10. Kambour RP, Klipfer HJ, Smith SA. Limiting oxygen indices of silicone block polymers. J Appl Polym Sci. 1981;26:847–59.

11. Alagar M, Thanikai Velan TV. Synthesis and characterization of high performance polymeric hybrid siliconized epoxy composites for aerospace applications. Mater Manuf Process. 1999;14:67–83.

12. Yuan DD, Yin HQ, Cai XF. Effect of a novel flame retardant containing silicon and nitrogen on the thermal stability and flame retardancy of polycarbonate. J Therm Anal Calorim. 2013;111:1531–7.

13. Chen XL, Hu Y, Song L. Thermal behaviors of a novel UV cured flame retardant coatings containing phosphorus, nitrogen and silicon. Polym Eng Sci. 2008;48:116–23.

14. Wang WJ, Perng LH, Hsiue GH, Chang FC. Characterization and properties of new silicone-containing epoxy resin. Polym. 2000;41:6113–22.

15. Liu SM, Lang XM, Ye H. Preparation and characterization of copolymerized aminopropyl/phenylsilsesquioxane microparticles. Eur Polym J. 2005;41:996–1001.

16. Chiang CL, Ma CCM. Synthesis, characterization, thermal properties and flame retardance of novel phenolic resin/silica nanocomposites. Polym Degrad Stab. 2004;83:207–14.

17. Qian XD, Song L, Yuan BH, Yu B. Organic/inorganic flame retardants containing phosphorus, nitrogen and silicon: Preparation and their performance on the flame retardancy of epoxy resins as a novel intumescent flame retardant system. Mater Chem Phys. 2014;143:1243–52.

18. Mariappan T, Yi DQ, Chakraborty A, Singha NK, Wilkie CA. Thermal stability and fire retardancy of polyurea and epoxy nanocomposites using organically modified magadiite. J Fire Sci. 2015;33:69–84.

19. Lewin M, Atlas SM, Pearce EM. Flame retardant polymeric materials. New York: Plenum Press; 1975.

20. Liu YL. Flame-retardant epoxy resins from novel phosphorus-containing novolac. Polym. 2001;42:3445–52.

21. Mercado LA, Galia' M, Reina JA. Silicon-containing flame retardant epoxy resins: synthesis, characterization and properties. Polym Degrad Stab. 2006;91:2588–94.

22. Wu ZJ, Li SC, Liu MJ, Wang Z. Liquid oxygen compatible epoxy resin: modification and characterization. RSC Adv. 2015;5:11325–33.

23. Ding JP, Tao ZQ, Zuo XB, Fan L, Yang SY. Preparation and properties of halogen-free flame retardant epoxy resins with phosphorus-containing siloxanes. Polym Bull. 2009;62:829–41.

24. Sun B, Liang GZ, Gu AJ, Yuan L. High performance miscible polyetherimide/bismaleimide resins with simultaneously improved integrated properties based on a novel hyperbranched polysiloxane having a high degree of branching. Ind Eng Chem Res. 2013;52:5054–65.

25. Gu AJ, Liang GZ. Thermal degradation behaviour and kinetic analysis of Epoxy/montmorillonitenano composites. Polym Degrad Stab. 2003;80:383–91.

26. Kanai H, Sullivan V, Auerback A. Impact modification of engineering thermoplastics. J Appl Polym Sci. 1994;53:527–41.

27. Kambour RP, Ligon WV, Russell RP. Enhancement of the limiting oxygen index of an aromatic polycarbonate by the incorporation of silicone blocks. J Polym Sci Part C Polym Lett. 1978;16:327–33.

28. Yuan DD, Deng LT, Yin HQ, Cai XF. Synergistic effect of organic silicon on the flame retardancy and thermal properties of PC/potassium-4-(phenylsulfonyl) benzenesulfonate (KSS) systems. J Appl Polym Sci. 2013;127:295–2101.

29. Wang X, Hu Y, Song L, Xing WY, Lu HD, Lv P, et al. Flame retardancy and thermal degradation mechanism of epoxy resin composites based on a DOPO substituted organophosphorus oligomer. Polym. 2010;51:2435–45.

30. Liu L, Chen X, Jiao C. Influence of ferrocene on smoke suppression properties and combustion behavior of intumescent flame-retardant epoxy composites. J Therm Anal Calorim. 2015;122(1):437–47.